ELSEVIER

New approach to determination of surface heterogeneity of adsorbents and catalysts from the temperature programmed desorption (TPD) technique: One step beyond the condensation approximation (CA) method

Piotr Kowalczyk [a], Katsumi Kaneko [a], Artur P. Terzyk [b,*], Hideki Tanaka [a],
Hirofumi Kanoh [a], Piotr A. Gauden [b]

[a] *Department of Chemistry, Faculty of Science, Chiba University, 1-3 Yayoi, Chiba 263, Japan*
[b] *Physicochemistry of Carbon Materials Research Group, Department of Chemistry, N. Copernicus University, Gagarin Street 7, 87-100 Toruń, Poland*

Abstract

Recovery of the desorption activation energy distribution from the experimental temperature programmed desorption (TPD) spectra is among the most difficult problems of adsorption science. Since the heterogeneity effects strongly influence on transport, diffusion, and catalytic reaction time, the estimation of their magnitude is very important for practical purposes. Up to the present, several theories have been used for the interpretation of the TPD results. Almost all advanced theoretical approaches take into account the effect of surface disorder (heterogeneity in desorption activation energy); however, they ignore the numerical difficulties coming from the "ill-posed" character of the linear Fredholm integral equations appearing in the theoretical description of the TPD results. Thus, there is a growing interest in developing novel methods supported by powerful numerical algorithms taking this into account. In the current study we propose a new approach and consider the theoretical aspect as well as numerical problems appearing in the TPD analysis. Our modeling is based on the well-known and generally accepted "absolute rate theory," which has been used extensively for the interpretation of TPD results. We propose and verify (applying computer simulations) the new advanced numerical hybrid type algorithms taking into account the heterogeneity effects. They seem to be very promising in TPD spectra analysis. The stability of the proposed advanced numerical methods is confirmed by the computer simulation experiments, and the results are compared with those obtained from the condensation approximation (CA) method.
© 2005 Elsevier Inc. All rights reserved.

Keywords: Temperature programmed desorption; Adsorption rate theory; Computer simulations

1. Introduction

Temperature-programmed desorption (TPD) techniques are important methods for the determination of the kinetics and thermodynamic parameters of desorption processes or decomposition reactions [1–4]. In a TPD experiment a sample is heated with a linear temperature increase and the partial pressures of desorbed molecules evolving from the sample are measured, usually by gas chromatography or mass spectrometry (Fig. 1). This is a simple view of much more complicated real processes associated with the TPD experiment. In reality the interpretation of the TPD spectrum (i.e., the desorption profile) is very difficult since diffusion and readsorption effects may influence the observed rate of desorption [5,6]. Moreover, most real systems are energetically heterogeneous and therefore they show a very complex TPD spectrum characterized by multiple peaks and shoulders [7]. These peaks are ascribed to various sites characterized by different activation energies for desorption. Obviously, heterogeneity effects are very important for practical

* Corresponding author.
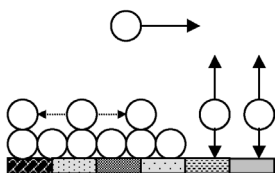 *E-mail address:* aterzyk@chem.uni.torun.pl (A.P. Terzyk).

Fig. 1. Schematic presentation of the TPD experiments from the heterogeneous surface. Open circles—preadsorbed molecules; dotted arrows—nearest-neighbor adsorbate–adsorbate interactions; solid line—desorption/readsorption from a homogeneous patch of the surface.

application of adsorbents, catalysts, and other materials [8]. In other words, it is important to obtain information about the strength and the composition of adsorption sites distributed on real solid surfaces [9]. So far, almost all theoretical studies of TPD have been based on the absolute rate theory (ART); however, the ART formulation for real existing more or less heterogeneous surfaces leads to a very difficult problem known in the literature as the "ill-posed" one [10–14]. Moreover, contrary to classical adsorption equilibrium theory, the TPD theory is more complicated since we have no explicit formula describing the rate of desorption from a homogeneous patch of a surface. Consequently, a theoretical development with advanced numerical algorithms should be proposed for the proper interpretation of the TPD results. Recently, Rudziński and co-workers [15] concluded that the so-called simplified condensation approximation (CA) methods, usually used on the ground of adsorption equilibrium theory, are in practice the only approximation methods leading to stable evaluation of the desorption activation energy from the TPD spectrum. It will be shown below that the CA gives only a general view of the real desorption activation energy and CA-type methods seem to be perfect as an initial approximation (i.e., trial function). It can be mentioned here that the CA method is often applied as the starting one in some advanced numerical algorithms [16,17] (for example in the HILDA algorithm) to evaluate the initial energy distribution function from the adsorption data.

It was established that ART does not explicitly give the coverage and temperature dependence necessary to predict TPD spectra in several systems. Thus an alternative model called statistical rate theory (SRT) was formulated [7, 18–21]. This theory was successfully developed mainly by Rudziński and Pańczyk [20,22]. Moreover the ART was criticized by Rudziński and Pańczyk [23], who showed, base on data on kinetics of CO_2 adsorption on scandia, that some of the ART parameters always exhibit a nonphysical meaning. On the other hand, different authors still prefer ART and this theory is still being developed [24–26]. Thus, in the present study we limit our considerations to the ART due to its simplicity.

Consequently, we propose a theoretical background and numerical algorithms for the proper estimation of desorption activation energy from TPD experiments. By analogy, in the developed algorithms the desorption activation energy obtained by means of the CA method is used as an initial approximation of the real one. Next, the real desorption acti-

vation energy is obtained from the Tikhonov's iterative regularization method (TIRM) [27–31] and from the weighted successive substitution algorithm (WSSA) [17–22]. The validity of the proposed theoretical approaches and numerical algorithms is confirmed by the simulation experiments. The proposed theoretical background, as well as the numerical hybrid-type methods, seem to be very excellent in the analysis of real surface heterogeneity by means of TPD experiments.

2. Problem formulation

According to the absolute rate theory (ART), the change of the surface coverage with time can be described as follows [32,33]:

$$\frac{d\theta(t)}{dt} = \Omega_a - \Omega_d$$
$$= A_a(\theta)p(1-\theta)^n \exp[-E_a/RT]$$
$$- A_d(\theta)\theta^n \exp[-E_d/RT]. \quad (1)$$

Here the first term describes the adsorption whereas the second describes the desorption rates. Both the adsorption and desorption preexponential factors (i.e., $A_a(\theta)$, $A_d(\theta)$, respectively) should be surface-coverage-dependent [34]. However, such dependence is not known exactly and probably its real formula is not simple. In Eq. (1) T is the temperature, p is the bulk pressure, R is the universal gas constant, and n denotes the number of adsorption sites in an elementary adsorption/desorption process. In other words, n describes the order of Eq. (1). As usual, $n = 1$ (i.e., one molecule occupies one adsorption site), at equilibrium $d\theta(t)/dt = 0$, and Eq. (1) with the assumption that $A_d(\theta) \equiv A_d$ and $A_a(\theta) \equiv A_a$ leads to the classical Langmuir isotherm [35]. Clearly, it is possible to introduce lateral interactions between adsorbed molecules by (for example) the Bragg–Williams approximation; however, in practice it is rather difficult to estimate the nearest-neighbor interaction energy [36,37]. For this reason Eq. (1) is usually assumed by the simplest Langmuir approximation.

Let us next assume that readsorption can be neglected and as a result the first term in Eq. (1) tends to zero:

$$A_a(\theta)p(1-\theta)^n \exp[-E_a/RT] \cong 0. \quad (2)$$

Moreover, as in the majority of papers dealing with the TPD results, we assume that the preexponential desorption factor slightly depends on the surface coverage and can be approximated by a constant value, $A_d(\theta) \cong A$ [38]. Finally, we are introducing a linear increasing of desorption temperature, $T = T_0 + \beta t$, and we transform Eq. (1) to the following final form:

$$\frac{d\theta(T)}{dT} = -\frac{A}{\beta}\theta^n \exp(-E_d/RT). \quad (3)$$

The nonlinear first-order differential equation given by Eq. (3) is known as the Polanyi–Wigner expression [39–41].

It has been frequently used for the description of the kinetics of thermodesorption from real solid surfaces [42–44].

It seems clear that Eq. (3) can be used only for the case of homogeneous surfaces. For real more or less heterogeneous surfaces the problem of the proper description of the kinetics of thermodesorption is more complicated [45,46]. Various methods have been applied for this purpose and they are commonly known as a "classical integral theory of adsorption" [17,47,48].

Let us assume that adsorption is localized. Additionally, we assume that all adsorption centers are grouped into noninteracting patches, each with the other "patches" (i.e., the "patch" model of a solid surface is assumed; see Fig. 1) [49]. Based on such assumption Eq. (3) should be treated as the kernel of the linear Fredholm integral equation of the first kind given by [10,50–52]

$$-\frac{d\theta(T)}{dT} = \int\limits_{\varXi(E_d)} \frac{A}{\beta}\theta^n \exp(-E_d/RT)\chi(E_d)\,dE_d. \qquad (4)$$

Here $\varXi(E_d) \in [E_{d,min}, E_{d,max}]$ denotes the physical region of E_d changing. The extension of the integration range to unphysical values is only a mathematical simplification, however; in real investigations it can lead to unexpected results characterized by some systematic errors [53–56].

From the physical point of view the differential distribution of adsorption sites $\chi(E_d)$ among corresponding values of the desorption energy E_d should be normalized, positive, and defined for the whole $\varXi(E_d) \in [E_{d,min}, E_{d,max}]$; thus [57,58]

$$\forall E_d: \quad \chi(E_d) \geqslant 0, \qquad (5)$$

$$\int\limits_{\varXi(E_d)} \chi(E_d) = 1. \qquad (5a)$$

The problem defined by Eq. (4), i.e., the inversion of the linear Fredholm integral equation of the first kind, is not trivial and belongs to the well-known "ill-posed" theory [59,60]. Moreover, the kernel in Eq. (4) is not given explicitly. The numerical methods such as the Euler (first-order Runge–Kutta) scheme, the second-order Runge–Kutta scheme, or the fourth-order Runge–Kutta scheme can be used for the evaluation of the Eq. (4) kernel [61]. It is worth emphasizing that all mentioned schemes are characterized by different stability and they always introduce some errors into the calculation results. As the result the inversion of Eq. (4) seems to be more difficult. However, as we show below, for some assumptions the explicit form of the Eq. (4) kernel can be obtained.

For the proper solution of ill-posed problems some special projected advanced numerical algorithms should be used. Among them Tikhonov's regularization is the most widespread and powerful [62–65]. Moreover, Eq. (4) can be simplified and solved by the so-called condensation approximation method (CA) [66]. However, the last method

replaces the kernel in Eq. (4) with an unphysical step function. As a result the mathematical problem is redefined, since the Fredholm-type integral equation is replaced by the Volltera one. From the Leibniz rule we can solve the Volterra type integral equation by differentiation [67]. Although this approach seems to be very simple and attractive one should remember that $\chi(E_d)$ obtained by means of the CA method can be regarded only as an approximation.

In the current study we propose two original advanced numerical algorithms based on the CA (initial approximation of $\chi(E_d)$) as well as on the iterative version of Tikhonov's zero-order regularization method and weighted successive substitution algorithm. Applying the numerical simulations we prove that the proposed algorithms can be used for the proper estimation of $\chi(E_d)$ from real noisy data with or without the nonnegativity constraint [68].

3. Numerical treatment

Let us assume that the desorption TPD obeys Langmuir behavior; i.e., $n = 1$. Thus the final linear Fredholm integral equation can be written as

$$-\frac{d\theta(T)}{dT} = \int\limits_{\varXi(E_d)} \frac{A}{\beta}\theta \exp(-E_d/RT)\chi(E_d)\,dE_d. \qquad (6)$$

It should be mentioned, that Eq. (6) is strongly simplified, compared to Eq. (1) (we assume that A is a constant, $n = 1$, and the first term is equal to zero). As a whole these assumptions restrict the use of the proposed approach because many desorption processes are not monomolecular, A is a function of temperature, and readsorption can play an important role in the TPD experiment if vacuum is not high. However, our approach is valid for a narrow TPD peak (desorption vs temperature) and for desorption of intact molecules.

Obviously the kernel in Eq. (6) (as we mentioned above) can be calculated by the different Runge–Kutta schemes; however, if we take under consideration the "ill-posed" character of Eq. (6) it seems not to be a good solution. It is easy to show that the well-known and the most accurate fourth-order Runge–Kutta scheme generates unstable results for $\theta \leqslant 0.001$. Obviously, it is connected with the numerical stability of the Runge–Kutta type methods. For such small values of the surface coverage the algorithm should automatically substitute zero.

Here we propose a different approach similar to that proposed by Bogillo and Shkilev (BS) [69]. Contrary to the BS approach (i.e., $\varXi(E_d) \in (0, \infty)$) we assume that the integration range in Eq. (6) is finite; i.e., $\varXi(E_d) \in [E_{d,min}, E_{d,max}]$.

Clearly, we can integrate the kernel in Eq. (6) and obtain

$$\ln(\theta) - \ln(\theta_0) = -\frac{A}{\beta}\int\limits_{T_0}^{T} \exp(-E/RT')\,dT'. \qquad (7)$$

Equation (7) can be integrated analytically and the final result is given by

$$\theta = \theta_0 \exp\left[\frac{AE_d}{\beta R} I(x_{\max}, x_{\min})\right], \tag{8}$$

where the integration boundaries are given by

$$x_{\min} = E_{d,\min}/(RT_0),$$
$$x_{\max} = E_{d,\max}/(RT). \tag{9}$$

The remaining functions appearing in Eq. (8) are defined as follows:

$$I = \int_{x_{\min}}^{x_{\max}} \frac{\exp(-x)}{x^2} \, dx$$
$$= \frac{\exp(-x_{\min})}{x_{\min}} - \frac{\exp(-x_{\max})}{x_{\max}}$$
$$+ E(-x_{\min}) - E(-x_{\max}). \tag{10}$$

Here the exponential integral can be obtained by the numerical integration scheme:

$$E(z) = -\int_{-z}^{\infty} \frac{\exp(-t)}{t} \, dt. \tag{11}$$

Equation (11) can be also solved by different methods.

Summing up, we obtain the explicit formula, i.e., Eq. (8), describing the kernel in Eq. (6). Obviously, the numerical integration of Eq. (11) is much more accurate and faster then the solution of the first-order nonlinear differential equation by Runge–Kutta type methods. This result is very important if we take into account that finally we want to solve the "ill-posed problem" defined by Eq. (6). Without any doubt, introduced errors in the kernel computation cause the increasing instability of the inversion of Eq. (6).

Up till now, we have developed the numerical recipes used for the computation of the Eq. (6) kernel. However, our final destination is to estimate the desorption energy distribution, $\chi(E_d)$, from the real noisy TPD data (i.e., the right-hand side, $-d\theta(T)/dT$, of Eq. (6)), by inversion of the linear Fredholm integral equation of the first kind given by Eq. (6). For this (the most important and difficult) purpose we developed two algorithms based on the advanced numerical methods. The first one is a combination of the CA and TIRM [70]. The second one is a combination of the CA and WSSA [71]. In the proposed algorithms the kernel in Eq. (6) can be calculated by the developed Eq. (8) or by different Runge–Kutta approximation schemes.

3.1. The CA method

The CA approach was introduced by Roginsky and used for the calculation of the adsorption energy distribution function from the single gas adsorption isotherm measured at subcritical conditions [72]. This approach is characterized by two main advantages; it gives stable results characterized by numerical simplicity.

In the proposed new algorithms we use the CA method for the evaluation of the first approximation of the real desorption activation energy distribution. It is hard to agree with the concept that the simple CA method can reproduce the real TPD from Eq. (6). However, it seems to be a perfect "trial function" used as a starting point for further more sophisticated algorithms well known from the "ill-posed" theory.

In the TPD theory the CA method was described in detail by Bogillo and Shkilev (BS) [69]. Let us consider the BS development since is very important for our proposal.

From the basic TPD theory the relation between the desorption activation energy and maximum temperature is known and given by

$$A \exp\left(-\frac{E_c}{RT}\right) = \frac{\beta E_c}{RT^2}. \tag{12}$$

Here $E_c \equiv E_d$ for the condensation point when the patch of the surface is spontaneously filled in the step fashion.

We can transform Eq. (12) by a simple transformation

$$\frac{E_c}{RT} = \ln\left(\frac{AT}{\beta}\right) - \ln\left(\frac{E_c}{RT}\right). \tag{13}$$

The distribution function $\chi(E_c)$ can be derived from Eq. (14)

$$\theta(T) = \int_{E_c}^{\infty} \chi(E_c) \, dE_c. \tag{14}$$

Obviously, from Eq. (14), it immediately follows that

$$\frac{d\theta}{dT} = \frac{d\theta}{dT} \frac{dT}{dE_c} \frac{dE_c}{dT}. \tag{15}$$

Next, let us introduce the function $F(T, E_c)$ such that

$$F = \frac{E_c}{RT} - \ln\left(\frac{AT}{\beta}\right) + \ln\left(\frac{E_c}{RT}\right). \tag{16}$$

The partial derivatives of this function with respect to T and E_c can be written as

$$\frac{\partial F}{\partial T} = -\frac{E_c}{RT^2} - \frac{2}{T} \quad \text{and} \quad \frac{\partial F}{\partial E_c} = \frac{1}{RT} + \frac{1}{E_c}. \tag{17}$$

Thus

$$\frac{dT}{dE_c} = -\frac{\frac{\partial F}{\partial E_c}}{\frac{\partial F}{\partial T}} = \frac{\frac{1}{RT} + \frac{1}{E_c}}{\frac{E_c}{RT^2} + \frac{2}{T}} = \frac{E_c + RT}{E_c - RT} \frac{RT^2}{E_c + 2RT}. \tag{18}$$

One can substitute $E_c/RT = x$. The derivative of T with respect to E_c can be written as

$$\frac{dT}{dE_c} = \frac{1+x}{R(2x + x^2)}. \tag{19}$$

One can calculate the function $\chi(E_c)$ from the single TDP spectrum (i.e., from the dependence of $d\theta/dT$ on T) in a very simple way, solving Eqs. (13) and (15).

Here we want to emphasize that the CA method always generates broader peaks than the real ones [73]. Moreover, when the peaks lie very close each to the other the CA method can detect the single peak [74]. On the other hand, the CA method always generates the TDP peaks in the correct desorption activation energy range and the general character of the heterogeneity effect is well predicted [47].

3.2. Tikhonov's iterative regularization method (TIRM)

The regularization type methods mathematically formulated by Tikhonov are the most powerful class of methods used on the ground of the "ill-posed" theory [29]. First, one can rewrite Eq. (6) in the operator form by the general method

$$Kx = y. \tag{20}$$

Here the matrix $K \in R^{mn}$, $m \geqslant n$, is the result of a kernel transformation by some quadrature, $y \in R^n$ is the right-hand side given by the experiment, and $x \in R^n$ is our unknown vector.

Unfortunately, Eq. (20) cannot be definitely solved by a simple elimination or by other similar numerical algorithms since the matrix K is ill-conditioned (i.e., its condition number is very high) [27].

For these types of problems the regularized minimization smoothing functional (or Tikhonov's functional) should be introduced,

$$x_\lambda = \min_x \left(\|Kx - y\|_2^2 + \lambda \|Lx\|_2^2 \right), \tag{21}$$

where $\|\zeta\|_2$ denotes 2-norm of vector ζ, λ is a positive number, usually called the Lagrange multiplayer or the regularization parameter controlling the degree of regularization. The operator L introduces the "static penalty" if x behaves undesirably. The simple choice is to let L be the identity matrix and hereby the regularization restricts the norm of x. Such a variant of regularization method is commonly known as a smoothing functional with zero-order stabilizing term.

It is easy to show that the solution of Eq. (21) leads to

$$x_\lambda = (K^*K + \lambda I)^{-1} K^* y, \tag{22}$$

where * denotes the transpose operation, I denotes the identity matrix, and $\lambda > 0$.

The real art of regularization lays in the proper selection of the regularization parameter λ [75]. Different methods have been proposed for the solution of this key problem; however, none of them can be treated as a general method. For this reason the scientists pay more attention to the iterative form of Eq. (22).

From the basic Tikhonov theory it is known that an alternative solution of Eq. (22) is given by [70]

$$K^* y + \lambda \zeta = A^* A + \lambda I, \tag{23}$$

where λ is arbitrarily chosen but relatively high value, say $\lambda = 10$, and $\zeta \in R^n$ is our initial approximation of the unknown vector y. Obviously, knowing these quantities we can solve Eq. (23) by the simple elimination algorithm or others, and as a result we obtain y from the initial guess, ζ. At the next step we substitute $\zeta = y$. The described iteration scheme is repeated M times. In practice, we start with an oversmoothed solution since $\lambda = 10$. During each iteration the solution rapidly changes and starts to approximate the real one precisely. Evidently, the number of iterations, M, can be treated as a regularization parameter. Consequently, the main difficulty here is connected with the proper selection of M, whereas this iteration scheme has some advantages compared with the classical regularization algorithm given by Eq. (22). We start with the initial guess which can be very close to the real unknown vector y. Our initial matrix is stable since λ is selected to be relatively high. The introduction of other constraints such as nonnegativity is very simple. We can control the iteration progress and changes in our solution in a very simple manner. As we show below the number of iterations, M, can be efficiently determined because it does not influence drastically on the final results. All mentioned above advantages of the iterative regularization method with the CA initial guess seem to be very suitable for the solution of the "ill-posed" problem defined by Eq. (6).

3.3. Weighted successive substitution algorithm (WSSA)

It is commonly known that regularization type methods are very useful in the field of the "ill-posed" problems. Moreover, other methods can be proposed for the solution of the concrete problem (here Eq. (6)). Since we have a good approximation given by the CA method, the WSSA method seems to be a very suitable algorithm for the proper solution of Eq. (6). The idea introduced in the WSSA algorithm is very simple. It is a successive improvement of the initial guess obtained by means of the CA. However, the theory of "ill-posed" problems indicates that the improvement should be performed very carefully.

Here we propose the simplest scheme. At first the stochastic hill-climbing procedure [75–80] is used for the creation of the new guess for y from the previous one (in the first iteration from the initial guess ζ). If the obtained new guess for y leads to the reduction of the measure of error between model and experimental data (i.e., sum of squared deviations or other), the new estimation for y is given by [31,71]

$$y^{j+1} = \omega y^{j+1} + (1 - \omega) y^j, \tag{24}$$

where j denotes iteration, and ω determines the relative weight of the old and new generations. The optimal value for ω can be found from the numerical experiments. The final number of iterations should be defined by the user, obviously, it can be found from the numerical experiments as well. What is the main advantage of Eq. (24)? Clearly, controlling the progress in improving the initial guess by a weighted scheme (given by Eq. (24)), we perform some kind of regularization, since we do not allow the model to

approach very close to the experimental data. Moreover, addition of constraints such as nonnegativity to Eq. (24) is very simple. As we show below, the proposed WSSA algorithm can be successfully applied for solving Eq. (6); however, the control of the constraints is more difficult than in the TIRM.

4. Simulation results and discussion

In the current section some results from the numerical experiments are used for the investigation of the stability of the two (above described) advanced numerical algorithms. As usual, the initial theoretical data were generated on the basis of an assumed desorption activation energy distribution function, i.e., $\chi(E_d)$ in Eq. (6), and other required parameters. Next, to the obtained right-hand sides in Eq. (6), different amounts of the Gaussian noise were added. Obviously, input data prepared in this way imitate the experimental ones.

For the proper representation of $\chi(E_d)$ we used several multimodal distribution functions. All were normalized to unity in the defined range of E_d change.

The first function can be used for imitation of the multimodal Gaussian bells and it can be written as

$$\chi(E_d) = \sum_{i=1}^{N} \frac{w_i \Pi_i}{\cosh[(E_d - \bar{E}_i)\delta_i]}, \tag{25}$$

where the normalization condition holds, i.e., $\sum_{i=1}^{N} w_i = 1$, N is the number of TPD peaks, w_i determines the weight of the ith base function, $\bar{E}_i$ denotes the position of the ith function maximum, and δ_i controls the width of the ith function. Clearly Π_i is given by

$$\Pi_i = \left(\frac{2}{\delta_i}\right)\left\{\text{arctg}\left[\exp\left(\delta_i E_{d,i}^{\max} - \delta_i \bar{E}_i\right)\right] - \text{arctg}\left[\exp\left(\delta_i E_{d,i}^{\min} - \delta_i \bar{E}_i\right)\right]\right\}. \tag{26}$$

Here $E_{d,i}^{\min}$ and $E_{d,i}^{\max}$ are the lower and upper activation desorption energies, respectively. The function given by Eq. (25) is very flexible and simple.

The second pseudo-function is modeled by the multimodal uniform distribution and can be written in general form as

$$\chi(E_d) = \sum_{i=1}^{N} \frac{w_i E_d}{E_{d,i}^{\max} - E_{d,i}^{\min}}. \tag{27}$$

Here the normalization condition, as well as all quantities, is the same as in the case of the first function.

The third function is the lognormal multimodal distribution similar to that introduced by Papenhuijzen and Koopal [81]:

$$\chi(E_d) = \sum_{i=1}^{N} \frac{w_i \sqrt{\alpha_i/\pi}}{\bar{E}_i \exp[1/(4\alpha_i)]} \exp\left\{-\alpha_i\left[\ln\left(E_d/\bar{E}_i\right)\right]^2\right\}. \tag{28}$$

As previously, $\sum_{i=1}^{N} w_i = 1$, N is the number of TPD peaks, $\bar{E}_i$ denotes the position of the ith function maximum, and α_i is a measure of the ith function width.

The last introduced function is the well-known bimodal Gaussian one given by the following formula:

$$\chi(E_d) = \frac{1}{\sqrt{\pi}}\left[\frac{w_1}{\sqrt{\beta_1}} + \frac{w_2}{\sqrt{\beta_2}}\right]^{-1}\left\{w_1 \exp\left[-\beta_1\left(E_d - \bar{E}_1\right)^2\right] + w_2 \exp\left[-\beta_2\left(E_d - \bar{E}_2\right)^2\right]\right\}. \tag{29}$$

Obviously, the normalization condition holds; i.e., $w_2 = 1 - w_1$; β_i, $i = 1, 2$, is a measure of the single Gaussian bell width, and E_i, $i = 1, 2$ is the position of the ith maximum.

In all computer experiments we use the same procedure. First we assume arbitrarily the heating rate constant $\beta = 2\ \text{K min}^{-1}$ and the preexponential factor $A = 10^6\ \text{min}^{-1}$. Here we want to mention that such values of the parameters are close to the experimental ones. Second, the simulated TPD profiles were obtained from Eq. (6) and applying one of the assumed activation desorption energy distributions (i.e., chosen from Eqs. (25)–(29)). Next, to the pure synthetic TPD profiles some measure of the Gaussian errors was added to imitate the experimental ones. Here, we assume that the absolute mean error, as a percentage given by

$$\varepsilon = \frac{100}{M}\left|\frac{\Theta_{\text{exp}} - \Theta_{\text{noisy}}}{\Theta_{\text{exp}}}\right|, \tag{30}$$

is equal to $\varepsilon \cong 6$. Here, Θ_{exp} denotes the pure generated data, and Θ_{noisy} are the noised ones. Obviously, the added error was scaled to the value of Θ_{exp}. It is worth emphasizing, that such added error is sufficiently high to imitate the real TPD experiments.

In Figs. 2 and 3 we present the proposed advanced numerical algorithms in action. At first, it is rather obvious that the simplified CA approach cannot be used for the estimation of the activation desorption energy distribution from the real noisy data. One should note that the CA always produces broader peaks (i.e., oversmoothed), suggesting higher heterogeneity effect then the real one is. However, the CA seems to be the perfect method for generating an initial approximation (i.e., trial function) for the unknown $\chi(E_d)$. As one can observe from Figs. 2 and 3, the CA is characterized by three advantages. The first is the simplicity. The second is that the obtained $\chi(E_d)$ (by means of the CA method) is placed within the proper range of E_d and the general picture is similar to the real one. The third advantage is that the CA is not sensitive to the value of the experimental errors (this is true only for relatively small errors—see below). What about the two remaining proposed algorithms? The TIRM works very well. Usually the small number of iterations leads to $\chi(E_d)$ being very close to the real one. Contrary to the simplified CA method, this type of regularization algorithm recovers the separated peaks well with intensity, position, and width close to the real ones. Like all regularization methods, the TIRM has a problem with discontinuous points. However, the assumption seems reasonable that nature produces
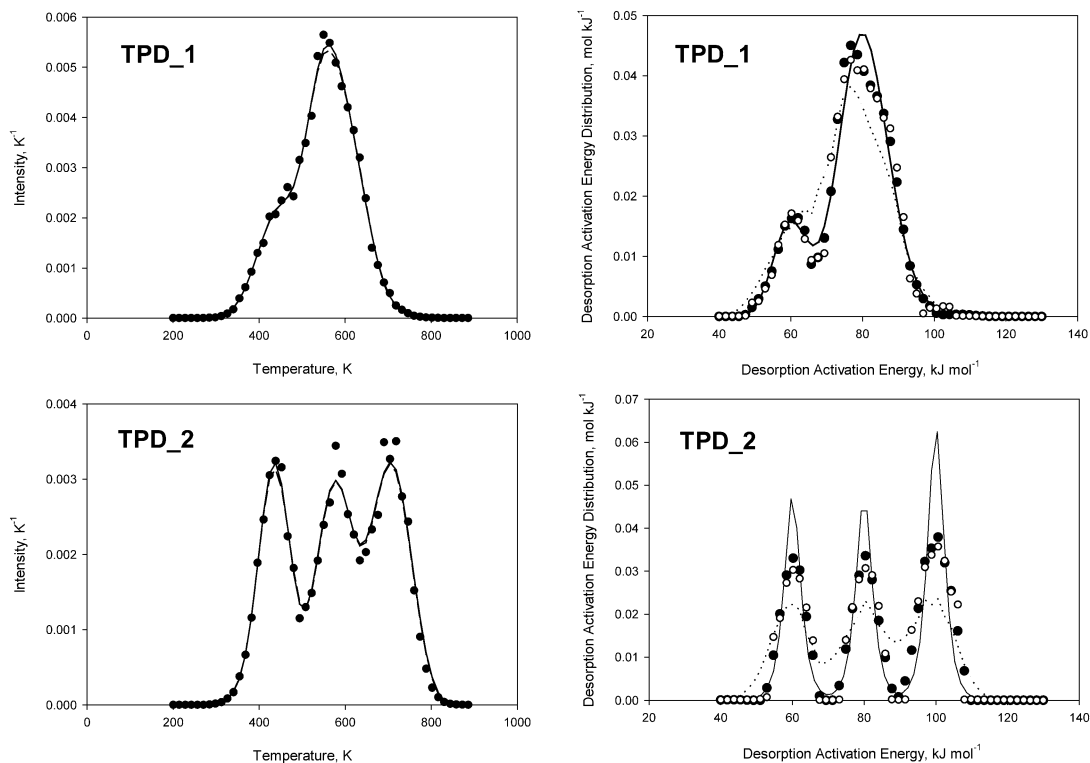
Fig. 2. Reconstruction of the TPD desorption activation energy distribution from noisy data. Left panel: black circles—noisy data; solid line—fitting by the TIRM algorithm; dashed line—fitting by the WSSA algorithm. Right panel: solid line—true $\chi(E_d)$; dotted line—recovery by the CA method; black circles—recovery by the TIRM algorithm; open circles—recovery by the WSSA algorithm.
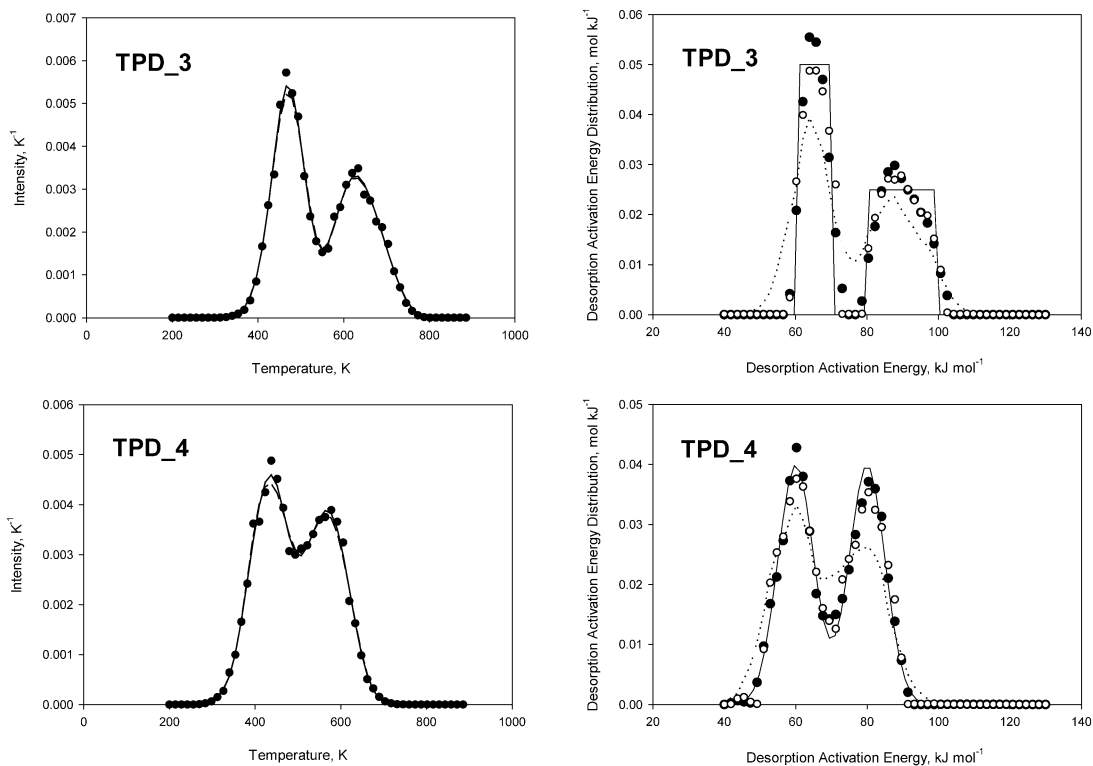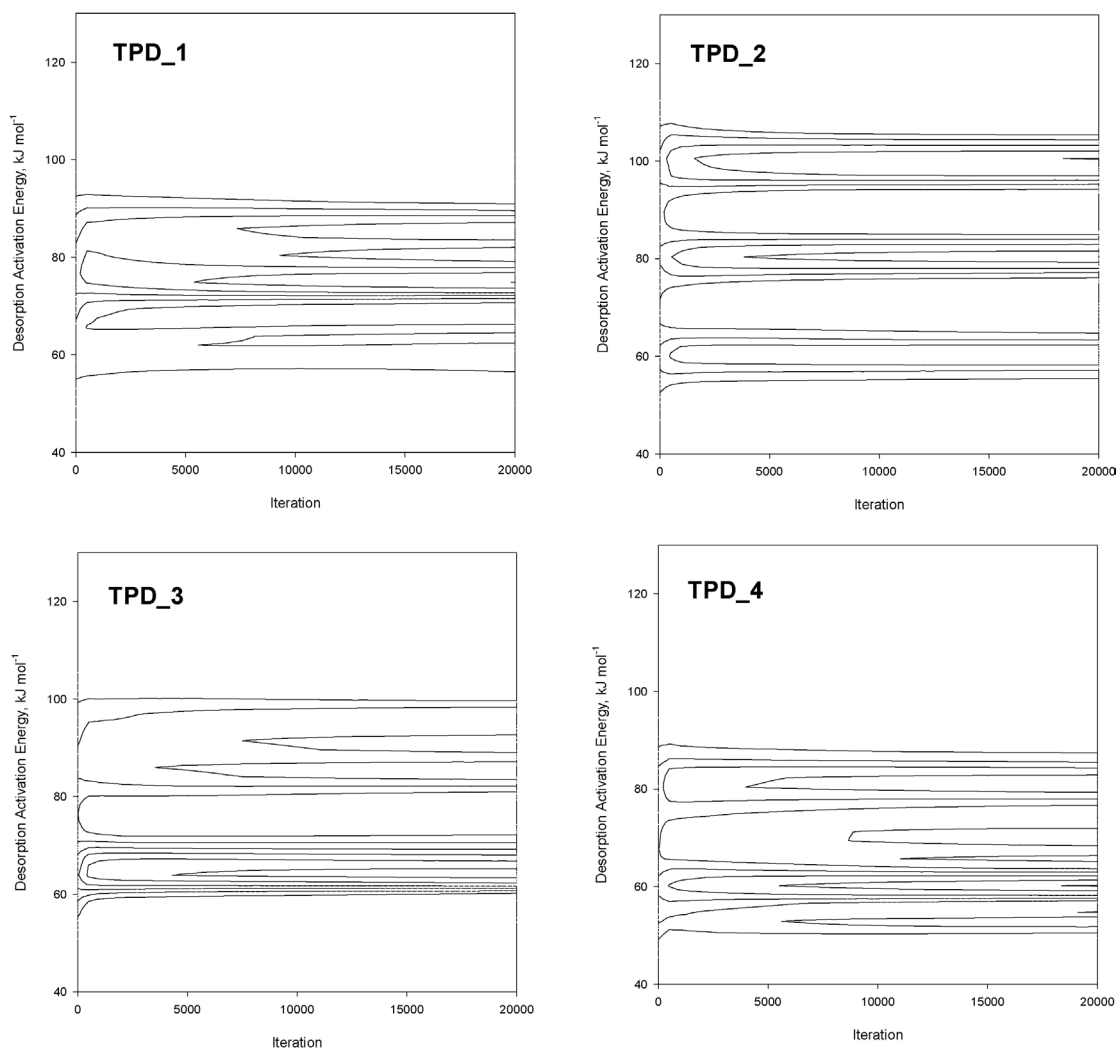

Fig. 3. The legend as in Fig. 2.

Fig. 4. The contour plots displaying the stability of the proposed TIRM algorithm.

smoothed curves, without discontinuous points. Additionally, the TIRM algorithm is very stable; i.e., the increasing number of iterations slightly influences the $\chi(E_d)$ (Fig. 4). Based on the results of our experiments we recommend this method for the analysis of experimental data.

The WSSA algorithm also gives very good recovery of the original $\chi(E_d)$ from the noisy data. The obtained results are very similar to the TIRM ones (Figs. 2 and 3). Obviously, the number of iterations in the WSSA is very important and can be treated as a regularization parameter. From the performed computer experiments we can conclude that the small number of iterations in the WSSA is appropriate for the recovery of original $\chi(E_d)$ from the noisy data. If the number of iterations increases some additional artificial peaks can appear. Evidently, this is connected with the "ill-posed" character of the considered problem. In the WSSA we do not apply any additional stabilizing terms as in the TIRM. The stability is achieved by the controlled weighted scheme given by Eq. (24). So the WSSA can recover the original $\chi(E_d)$ very well; however, the control of the obtained results is more difficult than in the TIRM (Fig. 5).

Summing up, this algorithm should be used more carefully than the TRIM; however, as for the TRIM, the final results provide its power.

Finally we present two additional advantages of the proposed algorithms. Fig. 6 shows data imitating the TPD spectra measured with very large error (bi-Gaussian distribution—Eq. (29) was assumed). From the recovered data it is seen that in this case the results of the CA method are strongly disturbed by the measurement error, while the TRIM as well as WSSA average the error and the recovered distributions are smoothed. The results from Fig. 7 are also very important. In this case we assumed that the peaks generated by the imitation of the multimodal Gaussian distribution (Eqs. (25) and (26)) lie very close (value of the error similar to that for the data in Figs. 2 and 3 was assumed). This assumption leads to the single TPD peak. As mentioned above, for this case the CA method recovers only one peak (Fig. 7). The TRIM algorithm works slightly better than the WSSA, and both proposed methods cope very well with the recovery problem (three peaks are observed). The evolution of the results of both presented methods for this
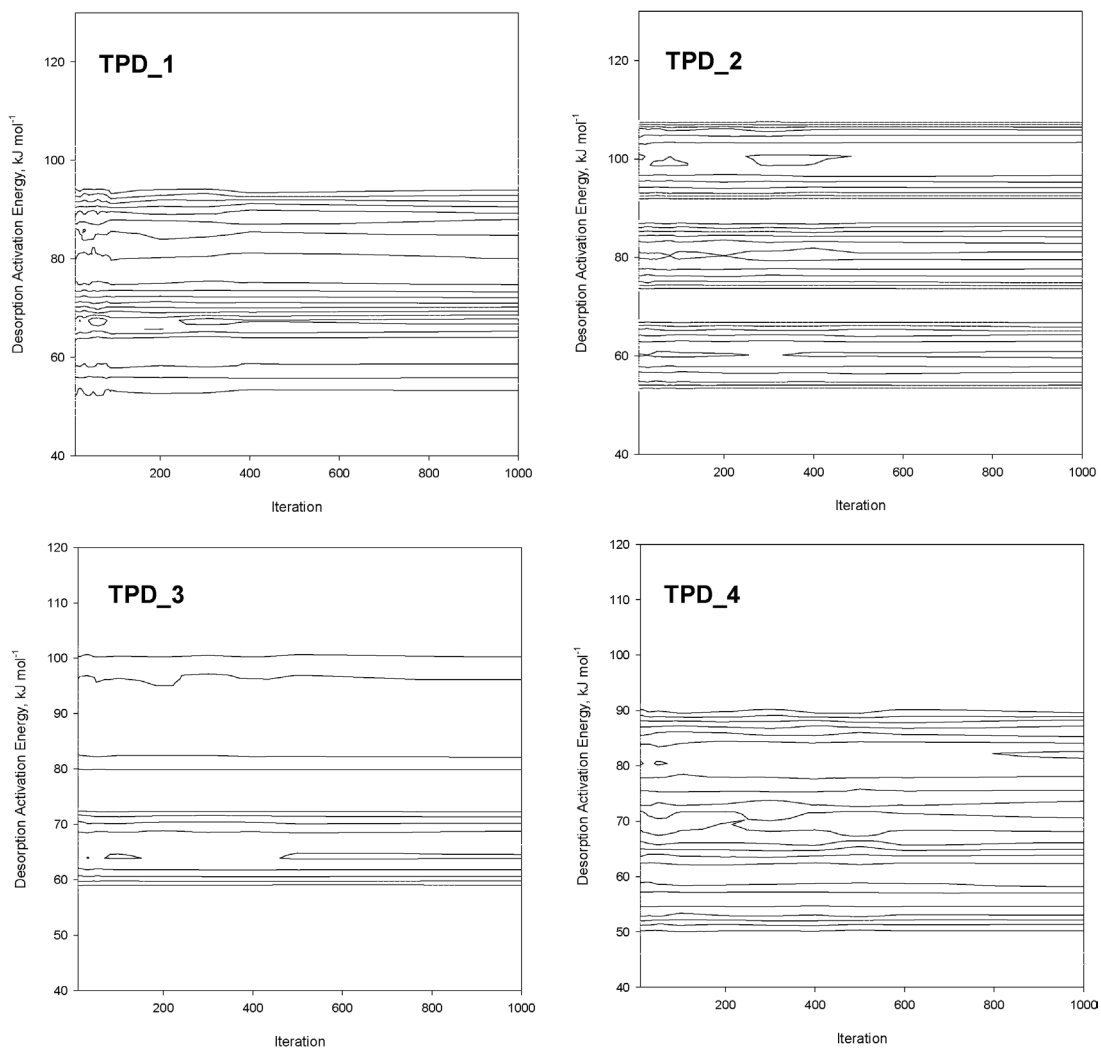
Fig. 5. The contour plots displaying the stability of the proposed WSSA algorithm.
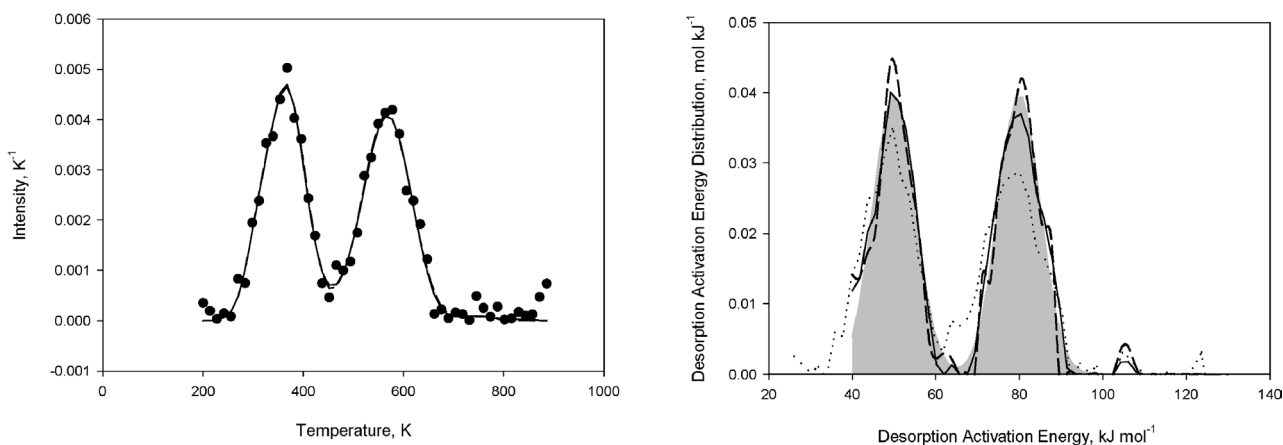

Fig. 6. The reconstruction of the TPD desorption activation energy distribution from the noisy data (very large error was assumed). Left panel: black circles—noisy data; solid line—fitting by the TIRM algorithm; dashed line—fitting by the WSSA algorithm. Right panel: gray area—true $\chi(E_d)$; dotted line—recovery by the CA method; solid line—recovery by the TIRM algorithm; dashed line—recovery by the WSSA algorithm.

problem is shown in Fig. 8. The results of the CA method (one peak) are the initial ones for both proposed advanced algorithms. The CA approach shows the presence of a single peak; however, with the increasing number of iterations, subpeaks emerge as the result of the new methods proposed in this study.
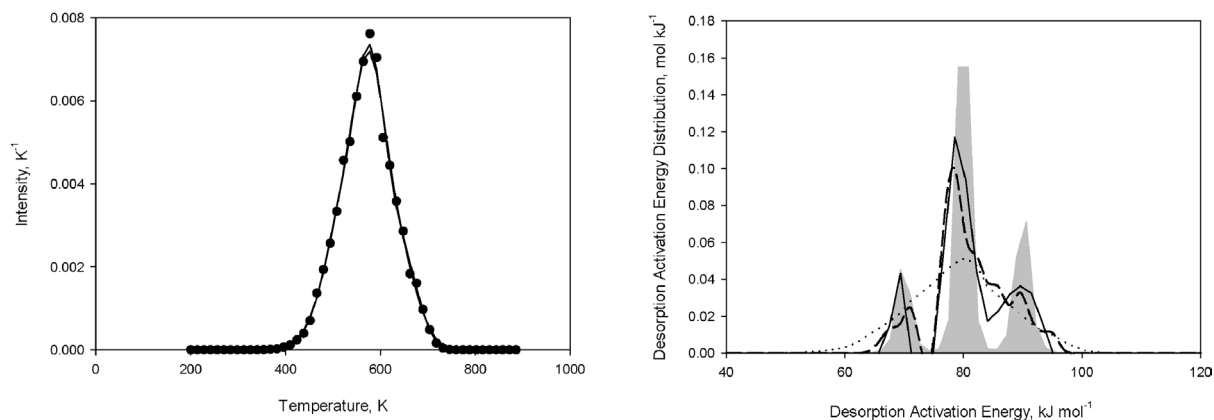
Fig. 7. The reconstruction of the TPD desorption activation energy distribution from the noisy data. Left panel: black circles—noisy data; solid line—fitting by the TIRM algorithm; dashed line—fitting by the WSSA algorithm. Right panel: gray area—true $\chi(E_d)$; dotted line—recovery by the CA method; solid line—recovery by the TIRM algorithm; dashed line—recovery by the WSSA algorithm.
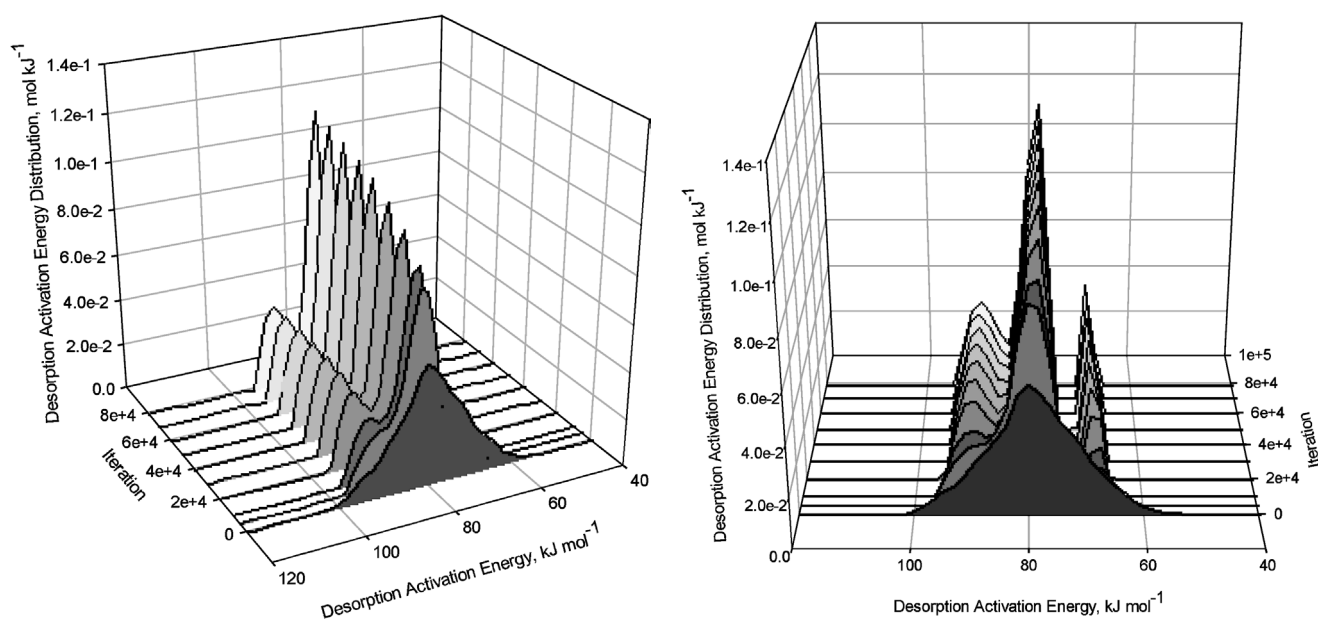

Fig. 8. The evolution of the solution obtained from the proposed algorithms with the progressing number of iterations. It is seen how from the initial distribution calculated by the CA method the assumed three-peak distribution emerges.

5. Conclusions

This paper shows the applicability of new procedures and related new algorithms for the study of the heterogeneity of adsorbents and catalysts. Basing on the ART theory we show how to solve the problem of recovering the distribution of the desorption energy. The power of the proposed methods and related new algorithms is demonstrated for series of simulated data disturbed by error, imitating experimental data. It seems that the TRIM method is the most powerful and hence it is recommended by us. The applicability of both algorithms for description of experimental data will be the subject of our future publications.

Acknowledgments

References

[1] Yu. Tovbin, in: W. Rudziński, W.A. Steele, G. Zgrablich (Eds.), Equilibria and Dynamics of Adsorption on Heterogeneous Solid Surfaces, Elsevier, Amsterdam, 1997.

[2] V.P. Zhdanov, Surf. Sci. Rep. 12 (1991) 183.

[3] W. Rudziński, T. Pańczyk, in: J. Schwarz, C. Contescu (Eds.), Surfaces of Nanoparticles and Porous Materials, Dekker, New York, 1998.

[4] M.D. Merchan, F. Salvador, J. Chem. Educ. 71 (1994) 1085.

[5] W. Rudziński, T. Borowiecki, A. Dominko, T. Pańczyk, Langmuir 13 (1997) 3445.

[6] Yu. Tovbin, E.B. Votyakov, Langmuir 9 (1993) 2652.

[7] F. Villeras, L.J. Michot, G. Gerard, J.M. Cases, W. Rudziński, J. Therm. Anal. Cal. 55 (1999) 511.

[8] F. Paulik, Special Trends in Thermal Analysis, Wiley, Chichester, 1995.

[9] T. Masuda, Y. Fujikata, S.R. Mukai, K. Hashimoto, Appl. Catal. A 165 (1997) 57.

[10] B. Hunger, M. von Szombathely, J. Hoffmann, P.J. Brauer, J. Therm. Anal. 44 (1995) 293.

[11] K. Koch, B. Hunger, O. Klepel, M.J. Heuchel, J. Catal. 172 (1997) 187.

[12] B. Hunger, M. von Szombathely, Stud. Surf. Sci. Catal. A 84 (1994) 669.

[13] H. Asada, Surf. Sci. 166 (1986) 271.

[14] H. Asada, Phys. Rev. B 37 (1988) 2223.

[15] W. Rudziński, T. Borowiecki, T. Pańczyk, A. Dominko, Adv. Colloid Interface Sci. 84 (2000) 1.

[16] L.K. Koopal, C.H.W. Vos, Colloids Surf. A 14 (1985) 87.

[17] M. Jaroniec, R. Madey, Physical Adsorption on Heterogeneous Solids, Elsevier, Amsterdam, 1988.

[18] J.A.W. Elliott, C.A. Ward, J. Chem. Phys. 106 (1997) 5677.

[19] C.A. Ward, J.A.W. Elliott, Appl. Surf. Sci. 196 (2002) 202.

[20] W. Rudziński, T.J. Pańczyk, J. Phys. Chem. B 104 (2000) 9149.

[21] W. Rudzinski, T. Borowiecki, T. Pańczyk, A. Dominko, J. Phys. Chem. B 104 (2000) 1984.

[22] W. Rudziński, T.J. Pańczyk, J. Phys. Chem. B 105 (2001) 6858.

[23] W. Rudziński, T.J. Pańczyk, Langmuir 18 (2002) 439.

[24] K. Miyabe, S. Takeuchi, J. Phys. Chem. B 101 (1997) 7773.

[25] K. Miyabe, G. Guiochon, Anal. Chem. 73 (2001) 3096.

[26] K. Miyabe, Anal. Chem. 74 (2002) 2126.

[27] P.C. Hansen, Rank-Deficient and Discrete Ill-Posed Problems, SIAM, Philadelphia, 1992.

[28] P.C. Hansen, Inverse Problems 8 (1992) 849.

[29] A.N. Tikhonov, V.Ya. Arsenin, Solution of Ill-Posed Problem, Winston, New York, 1997.

[30] V.A. Morozov, Methods for Solving Incorrectly Posed Problems, Springer-Verlag, Berlin, 1984.

[31] H. Tanaka, Molecular Confinement in Nanopores, Thesis, Graduate School of Science and Technology, Chiba University, 2002.

[32] A. Clark, The Theory of Adsorption and Catalysis, Academic Press, New York, 1970.

[33] Yu. Tovbin, Theory of Physical Chemistry Processes at a Gas–Solid Interface, CRC Press, Boca Raton, FL, 1991.

[34] F.D. Nieto, D.L. Valladares, P.A. Velasco, G. Zgrablich, J. Phys. Condens. Matt. 5 (1993) A147.

[35] W. Rudziński, T. Borowiecki, A. Dominko, T. Pańczyk, J. Grylicki, Pol. J. Chem. 72 (1998) 2103.

[36] S. Bhatia, I. Beltramini, D.D. Do, Catal. Today 8 (1990) 309.

[37] J. Cortes, E. Valencia, P. Araya, J. Chem. Phys. 100 (1994) 7672.

[38] G.F. Cerofolini, N.J. Re, J. Colloid Interface Sci. 174 (1995) 428.

[39] P.A. Redhead, Vacuum 12 (1962) 203.

[40] H.G. Karge, V.J. Dondur, J. Phys. Chem. 94 (1990) 765.

[41] E. Tomkova, Surf. Sci. 351 (1996) 309.

[42] H.G. Karge, E.P. Boldingh, Catal. Today 3 (1988) 379.

[43] H.G. Karge, E.P. Boldingh, Catal. Today 3 (1988) 53.

[44] M. Jackel, F. Fietzke, Vacuum 44 (1993) 421.

[45] M.A. Ferro-Garcia, J.P. Joly, J. Rivera-Utrilla, C. Moreno-Castilla, Langmuir 11 (1995) 2648.

[46] A. Dandekar, R.T.K. Baker, M.A. Vannice, Carbon 36 (1998) 1821.

[47] W. Rudziński, D.H. Everett, Adsorption of Gases on Heterogeneous Surfaces, Academic Press, New York, 1992.

[48] D.D. Do, Adsorption Analysis: Equilibria and Kinetics, Imperial College Press, London, 1998.

[49] S. Ross, J.P. Oliver, On Physical Adsorption, Interscience, New York, 1964.

[50] B. Hunger, S. Matysik, M. Heuchel, W.D. Einicke, Langmuir 13 (1997) 6249.

[51] B. Hunger, M. von Szombathely, Z. Phys. Chem. 190 (1995) 19.

[52] I.A. Beta, B. Hunger, H. Bohlig, J. Therm. Anal. 64 (2001) 1191.

[53] P.A. Gauden, Theoretical Description of the Structural and Energetic Heterogeneity of Carbonaceous Materials, Thesis, UMK, Toruń, 2001, in Polish.

[54] P.A. Gauden, A.P. Terzyk, J. Colloid Interface Sci. 227 (2000) 482.

[55] P.A. Gauden, A.P. Terzyk, Theory of Adsorption in Micropores of Carbonaceous Materials, WICHiR, Warsaw, 2002, in Polish.

[56] A.P. Terzyk, P.A. Gauden, G. Rychlicki, R. Wojsz, Langmuir 15 (1999) 285.

[57] G.F. Cerofolini, N. Re, Riv. Nuovo Cimento Soc. Ital. Fis. 16 (1993) 1.

[58] P. Kowalczyk, A.P. Terzyk, P.A. Gauden, Langmuir 18 (2002) 5406.

[59] A.N. Tikhonov, A.V. Goncharskii, V.V. Stepanov, A. Yagola, Regularization Algorithms and a Priori Information, Nauka, Moscow, 1983, in Russian.

[60] P. Merz, J. Comput. Phys. 38 (1980) 64.

[61] W.H. Press, S.A. Teukolsky, W.T. Vetterling, B.P. Flannery, Numerical Recipes in Fortran, Cambridge Univ. Press, Cambridge, UK, 1992.

[62] P.C. Hansen, BIT 27 (1987) 534.

[63] M. Hanke, BIT 36 (1996) 287.

[64] D.L. Phillips, J. Assoc. Comput. Mach. 9 (1962) 84.

[65] K. Miller, SIAM J. Math. Anal. 1 (1970) 52.

[66] V.I. Bogillo, P. Staszczuk, J. Therm. Anal. Cal. 55 (1999) 493.

[67] I.N. Bronsztejn, K.A. Siemiendiajew, Mathematics—The Encyclopedic Handbook, PWN, Warsaw, 1986, in Polish.

[68] J. Jagiello, Langmuir 10 (1994) 2778.

[69] V.I. Bogillo, V.P. Shkilev, J. Therm. Anal. Cal. 55 (1999) 483.

[70] C.T.H. Baker, The Numerical Treatment of Integral Equations, Clarendon, Oxford, 1977.

[71] P. Tarazona, Phys. Rev. A 31 (1985) 2672.

[72] S.Z. Roginsky, Dokl. Akad. Nauk SSSR 45 (1944) 61.

[73] L.K. Koopal, M.M. Nederlof, W.H. van Riemsdijk, P.A. Barneveld, Langmuir 13 (1997) 961.

[74] M.M. Nederlof, W.H. van Riemsdijk, L.K. Koopal, Environ. Sci. Technol. 28 (1994) 1048.

[75] P.A. Gauden, P. Kowalczyk, A.P. Terzyk, Langmuir 19 (2003) 4253.

[76] Z. Michalewicz, Genetic Algorithms + Data Structures = Evolution Programs, Springer-Verlag, Berlin, 1996.

[77] A.P. Terzyk, P.A. Gauden, P. Kowalczyk, Carbon 40 (2002) 2879.

[78] P. Kowalczyk, L. Solarz, A.P. Terzyk, P.A. Gauden, V. Gun'ko, Shedae Informaticae MCCLIX (2002) 75.

[79] P. Kowalczyk, A.P. Terzyk, P.A. Gauden, R. Leboda, E. Szmechtig-Gauden, G. Rychlicki, Z. Ryu, H. Rong, Carbon 41 (2003) 1113.

[80] P. Kowalczyk, V.M. Gun'ko, A.P. Terzyk, P.A. Gauden, H. Rong, Z. Ryu, D.D. Do, Appl. Surf. Sci. 206 (2003) 67.

[81] J. Papenhuijzen, L.K. Koopal, in: R.H. Ottewill, C.H. Rochester, A.L. Smith (Eds.), Adsorption from Solution, Academic Press, London, 1983.